Article

Not peer-reviewed version

Targeting Extracellular RNA Mitigates Hepatic Lipotoxicity and Liver Injury in NASH

Archana Tewari , Sangam Rajak , Sana Raza , Pratima Gupta , Bandana Chakravarti , Jyotika Srivastava , Chandra Prakash Chaturvedi , Rohit Anthony Sinha *

Posted Date: 20 June 2023

doi: 10.20944/preprints202306.1436.v1

Keywords: NASH; Lipotoxicity; NAFLD; extracellular RNA; RNase1; TLR3

Article

Targeting Extracellular RNA Mitigates Hepatic Lipotoxicity and Liver Injury in NASH

Archana Tewari [1], Sangam Rajak [1], Sana Raza [1], Pratima Gupta [1], Bandana Chakravarti [1], Jyotika Srivastava [2], Chandra P Chaturvedi [2] and Rohit A. Sinha [1,*]

[1] Department of Endocrinology, Sanjay Gandhi Postgraduate Institute of Medical Sciences, Lucknow, India
[2] Stem Cell Research Facility, Department of Hematology, Sanjay Gandhi Postgraduate Institute of Medical Sciences, Lucknow, India
* Correspondence: anthony.rohit@gmail.com; rasinha@sgpgi.ac.in

Abstract: Non-alcoholic steatohepatitis (NASH) is a clinically serious stage of non-alcoholic fatty liver disease (NAFLD). Histologically characterized by hepatocyte ballooning, immune cell infiltration and fibrosis, NASH, at a molecular level involves lipid induced hepatocyte death and cytokine production. Currently, there are very few diagnostic biomarkers available to screen NASH, and no pharmacological intervention is available for its treatment. In this study, we show that hepatocyte damage by lipotoxicity results in the release of extracellular RNAs (eRNAs) which serve as damage-associated molecular patterns (DAMPs) that stimulate the expression of pro-apoptotic and pro-inflammatory cytokines, aggravating inflammation, and cell death in HepG2 cells. Furthermore, the inhibition of eRNA activity by RNase 1 significantly increased cellular viability and reduced NF-kB mediated cytokine production. Similarly, RNase 1 administration significantly improved hepatic steatosis, inflammatory and injury markers in a murine NASH model. This study, therefore, for the first time, underscores the therapeutic potential of inhibiting eRNA action as a novel strategy for NASH treatment.

Keywords: Damage associated molecular patterns (DAMPs); extracellular RNA; lipotoxicity; inflammation; non-alcoholic steatohepatitis (NASH)

1. Introduction

Non-alcoholic fatty liver disease (NAFLD) refers to a spectrum of liver conditions affecting people who drink little to no alcohol [1]. This ranges from benign hepatic fat deposition (steatosis) to a much severe condition known as non-alcoholic steatohepatitis (NASH) [2]. NASH is a clinically alarming stage of NAFLD which results in liver injury, fibrosis, cirrhosis, and may eventually culminate into hepatocellular cancer (HCC) [2]. Unfortunately, we have no approved drug therapy for NASH and its progression may become irreversible in some individuals.

Hepatic injury due to lipotoxicity associated with NASH, is triggered by lipids which include saturated free fatty acids such as palmitic acid (PA) [3]. Upon entry into the hepatocytes, PA induces a number of cellular derangements including activation of stress kinases, oxidative stress, mitochondrial dysfunction, [4] and eventually, cell lysis [5,6]. The death of hepatocytes caused by lipotoxicity results in the release of a variety of damage-associated molecular patterns (DAMPs) such as DNA fragments, histones, ATP, uric acid, and cholesterol crystals, that act as stress signals to activate DAMP receptors, such as toll-like receptors (TLRs), purinoreceptors (P2X and P2Y) and C-type lectin domain (CLEC)12A, thereby initiating sterile inflammation and exacerbating tissue injury in NASH [7–12]. Extracellular RNA (eRNA) also belongs to this heterogeneous group of DAMPs and includes several types of RNAs present in the extracellular environment, including microRNA (miRNA), transfer RNA (tRNA), small interfering RNA (siRNA), and long noncoding RNA (lncRNA) [13]. eRNA released as a result of tissue injury may play a role in differentiation, chromatin modification, and inflammation, as well as tissue injury and repair [13–21]. eRNA binds to the Toll-

 doi:10.20944/preprints202306.1436.v1

like receptor (TLR) family receptors to induce apoptosis and inflammation in diseases such as ischemia-reperfusion and sepsis injury in cardiomyocytes [22–24]. Consistently, the administration of Ribonuclease1 (RNase 1), which degrades eRNA, has shown efficacy in decreasing disease severity in several preclinical disease models [22–24]. However, it is unknown whether eRNA plays a role in hepatic cell injury and pro-inflammatory cytokine production in NASH and whether RNase 1 administration can act as an interventional strategy to reduce NASH progression.

Here in this study, we demonstrate that eRNA released from injured/dead hepatocytes upon lipotoxic insult, increases hepatic injury along with pro-inflammatory cytokine production. Furthermore, the degradation of eRNA by RNase 1 treatment attenuates lipotoxicity both *in vitro* and in a mouse model of NASH.

2. Materials and Methods

2.1. Cell culture and treatment

HepG2 and AML12 hepatic cells were procured from American Type Culture Collection (ATCC, Manassas, VA, USA). HepG2 cells were cultured in DMEM supplemented with 10% fetal bovine serum (FBS) and 1% penicillin/streptomycin. Mouse hepatocytes, AML12 cells (CRL-2254) were maintained in DMEM-F12 1:1 containing 10% FBS, 1x ITS (Thermo Fisher Scientific, 41400), 10 nM dexamethasone and 1x penicillin/streptomycin. Both cell lines were maintained at 37°C in presence of 5% CO2. At 80% confluence, lipotoxicity was induced into the cells using 0.75 mM PA (saturated fatty acid), dissolved in ethanol; 0.5% BSA was used as a carrier for PA. Cells in the vehicle group were given only ethanol in 0.5% BSA containing media. For the administration of RNase 1, cells were incubated with 2.8U/mL RNase 1, one hour prior to the addition of PA and the treatment was continued upto 24 hours to maintain a sustained release of RNase 1 (Invitrogen, #12091021) in the culture media.

2.2. MTT assay

HepG2 and AML12 cells ($1x10^4$) seeded into 96 well plates, were treated with PA with and without RNase 1. Vehicle control cells were given only ethanol in 0.5% BSA containing media. After 24 hours of treatment, medium was supplemented with MTT reagent (5mg/ml) for 4 hours at 37°C. DMSO (100ul) was then added to dissolve the purple formazan crystals and the plate was shaken for 10 min. Absorbance was recorded at 570nm using a multi-well spectrophotometer (ELISA reader).

MTT assay was also performed in HepG2 cells treated with PA in presence and absence of 10uM of TLR3/dsRNA complex inhibitor (Merck, #614310). In this case, cells in the vehicle group received both DMSO and ethanol in 0.5% BSA containing media as the TLR3/dsRNA complex inhibitor was dissolved in DMSO.

2.3. Analysis of total eRNA levels

Total eRNA levels in the conditioned media from vehicle control, PA treated, and PA+RNase 1 treated HepG2 cells were analyzed using the eRNA quantitation kit (Promega, Cat No: E3310 QuantiFluor® RNA System), according to the manufacturer's protocol, using a multimode reader.

2.4. Oil Red O Staining

Lipid droplets in HepG2 cells were assayed by Oil Red O Stain. 96 well plates containing HepG2 cells were washed twice with phosphate-buffered saline. Cells were fixed with 10% paraformaldehyde for 30 min. After this, cells were washed with distilled water and 60% isopropanol was added for 5 minutes. Cells were then incubated in Oil Red O stain for 20 minutes, followed by washing with distilled water to remove the excess stain. Next cells were incubated with Hematoxylin for 1 minute. Oil Red O stain was extracted with 100% isopropanol for 5 minutes and absorbance was recorded at 492 nm using a multi-well spectrophotometer (ELISA reader).

 doi:10.20944/preprints202306.1436.v1

2.5. Animal experiments

HFMCD NASH Model: 6-8-weeks-old male C57BL/6N mice were fed with a high-fat methionine-choline-deficient (HFMCD) diet consisting of 60 kcal% fat and 0.1% methionine by weight (A06071302; Research Diets, New Brunswick NJ), littermate mice fed with normal chow diet (NCD) were used as control mice. Mice were divided into three groups: NCD, HFMCD diet alone for 4 weeks, and HFMCD with RNase 1 (50ug/kg). RNase1 was injected intra-peritoneally, starting every alternate day after 2 weeks feeding on HFMCD diet, and continued for the next 2 weeks. All the animals were sacrificed after 4 weeks, and serum and liver tissues were collected. All animal procedures were carried out in accordance with the institutional guidelines for animal research at SGPGIMS.

2.6. RNA isolation and qRT-PCR

Total RNA from mice liver tissues and HepG2 cells was isolated using Trizol reagent (#343909). qRT-PCR was performed using the QuantiTect SYBR Green PCR Kit (Qiagen, 204141) according to manufacturer's instructions. The GAPDH gene was used for normalization. KiCqStart SYBR Green Primers were purchased from Sigma-Aldrich, United States. Primer IDs were, Mouse Tnf-alpha (M_Tnf_1),Mouse IL6(M_IL6_1), Mouse IL1 beta (M_IL 1 beta _1), Mouse CCL20 (M_CCL20_1), Mouse Ccl2 (M_Ccl2_1), Mouse Ccl3 (M_Ccl3_1), Mouse Cxcl10 (M_Cxcl10_1), Mouse GAPDH (M_ Gapdh_1), Human Tnf- alpha (H_Tnf_1), Human IL-6 (H_IL6_1) Human CCL3(H_CCL3L3_1), Human CXCL10 (H_CXCL10_1), Human CCL20 (H_CCL20_1) and Human GAPDH (H_Gapdh_1).

2.7. Western blotting

HepG2 cells and mice liver tissue samples were lysed using RIPA buffer (Sigma, #R0278) mixed with phosphatase and protease inhibitor cocktails. Fifty microgram of protein was subjected to sodium dodecyl sulfate—polyacrylamide gel electrophoresis and electro-transferred onto a nitrocellulose membrane as per the manufacturer's guidelines (Bio-Rad Laboratories, United States). Image acquisition was done using ChemiDoc (Syngene Model No: -G: BOX CHEMIXRQ). Densitometry analysis was performed using ImageJ software (NIH, Bethesda, MD, United States). Antibodies used were anti-GAPDH (Cell Signaling Technology, # 5174), anti- F4/80 (Cell Signaling Technology, # 70076), anti-Cleaved PARP (Cell Signaling Technology,#5625), anti-Phospho-c-JUN (Cell Signaling Technology,#3270), anti-Phospho-p-38MAPK (Cell Signaling Technology,#4511), anti-Phospho-SAPK/JNK(Cell Signaling Technology,#4668), anti-JNK (Cell Signaling Technology,#9252), anti-c-JUN(Cell Signaling Technology,#9165), anti-p-38MAPK(Cell Signaling Technology,#8690), anti-LC3B(Cell Signaling Technology,#2775) and anti-P62(Cell Signaling Technology,#39749).

2.8. H&E staining

Tissues from the liver were fixed in situ after opening the abdomen, immersed in 4% paraformaldehyde in PBS, and processed into paraffin blocks. Sections were sliced at 5-micron thickness and mounted on slides to perform H&E staining. Images were analyzed using the ImageJ software, NIH. The non-alcoholic fatty liver disease activity scoring (NAS) system was used to quantify steatosis (0–3), lobular inflammation (0–3), and hepatocellular ballooning (0–2). Liver biopsies scored NAS ≥5 were classified as definitive NASH [25].

2.9. Serum ALT test

Alanine aminotransferase (ALT) levels in the serum were assessed using the kit (Abcam calorimetric assay kit #ab105134) as per the manufacturer's protocol.

2.10. Liver TG analysis

Liver triglyceride (TG) levels were assessed using the kit (Cayman, Triglyceride Colorimetric assay kit # Cat No. 10010303) as per the manufacturer's protocol.

 doi:10.20944/preprints202306.1436.v1

2.11. Confocal microscopy

Immunofluorescence experiments were performed on treated HepG2 cells in chambered slides and in paraffin-embedded sections of mouse liver. In brief, formalin-fixed cells and tissues were permeabilized with 0.1% Triton X-100 (SIGMA-ALDRICH, X100) in PBS for 5-10 min and blocked with 3% BSA-PBS for 30 min, at room temperature. Cells and tissues were incubated with the primary antibody (1:200 in 3% BSA-PBS) overnight at 4°C followed by fluorochrome labelled secondary antibodies (Molecular probes) and cell imaging was performed using an LSM710 Carl Zeiss (Carl Zeiss Microscopy GmbH, Germany) confocal microscopy. The primary antibody used for HepG2 cells and liver sections was anti-NFkB (Cell Signaling Technology, #8242). Colocalization studies were performed using ImageJ software with JACoP plugin.

2.12. Mitochondrial ROS detection

Mitochondrial ROS was detected in vehicle control and treated HepG2 cells using 5 μM MitoSOX™ Red (catalog number #M36008), in which cells were incubated for 20-30 min at 37°C. After washing with PBS, reading was taken in a fluorimeter at an excitation wavelength of 510 nm and an emission wavelength of 580 nm.

2.13. Mitochondrial membrane potential (MMP)

Mitochondrial membrane potential (MMP) was assessed by JC-1 staining. HepG2 cells seeded into 96 well black bottom plates were treated with PA with and without RNase 1 for 24 hours. Cells were washed with PBS and incubated with 2 μM JC-1 dye (Invitrogen, catalog number #T3168) at 37 °C for 30 min. Fluorescence was measured by a fluorimeter (Synergy HTX multimode microplate reader, BioTek) at an excitation wavelength of 488 nm and an emission wavelength of 530 nm (monomer) and 590nm (aggregates). Loss of MMP was calculated from the ratio of emission wavelength at 590nm/530nm.

2.14. Statistics

One-way ANOVA with Tukey's post hoc test was used to compare among groups. Statistical analysis was performed using the Graph-Pad Prism software, version 5.0. *$p < 0.05$, **$p < 0.01$, and ***$p< 0.001$ were considered statistically significant.

3. Results

3.1. RNase 1 attenuates PA induced cellular injury in HepG2 cells

Lipotoxicity by PA is known to induce apoptosis and cellular stress in hepatic cells, and mimics hepatocyte damage in NASH [26]. To determine if PA induced hepatocyte injury leads to the release of eRNA, we assessed the eRNA content in the conditioned media of PA treated HepG2 cells and observed a significant increase in the eRNA levels. Furthermore, the co-administration of RNase 1 significantly reduced the released eRNA levels upon PA treatment, when compared with PA treatment alone **(Figure 1A)**. Concurrently, RNase 1 treatment also significantly rescued the cellular viability of HepG2 upon lipotoxic insult **(Figure 1B)**. These results were further supported by the decrease in cleaved PARP levels (apoptosis marker) in RNase 1 and PA treated cells, compared to increased apoptosis, as observed in PA alone treated cells **(Figure 1C, D)**. Additionally, PA induced hepatic steatosis was also reduced by RNase 1 administration **(Supplementary Figure 1)**. Cellular stress kinases such as p-JNK and p-p38MAPK are key mediators of PA induced cellular stress [27]. In line with these observations, we also assessed the effect of RNase 1 treatment on PA induced JNK and p38MAPK activation. Our results showed that, indeed, similar to its effect on cellular viability, the targeted degradation of eRNA by RNase 1 significantly reduced the PA induced activation of JNK, its downstream target c-jun, and p38MAPK **(Figure 1 E-J)**. Furthermore, Rnase 1 treatment also rescued PA induced autophagy block which is a major mediator of lipotoxicity [28] **(Supplementary Figure 2).** To verify if the observed effects of RNase 1 are specifically due to its effects on eRNA, we

Preprints (www.preprints.org) | NOT PEER-REVIEWED | Posted: 20 June 2023 doi:10.20944/preprints202306.1436.v1

also used a pharmacological inhibitor of TLR3, a receptor of eRNA and observed a similar rescue effect on PA induced cell death **(Figure 1K)**. This small molecule inhibitor specifically inhibits the TLR3/dsRNA complex formation and has been shown to prevent eRNA signaling [29]. Concurrently, the administration of RNase 1 alone to HepG2 cells had no effect on cell viability **(Supplementary Figure 3A)**. These sets of results, thus, rule out any possible off target effect of RNase 1. We further validated the effect of RNase 1 on another hepatocyte cell line (AML-12) and observed similar effects as observed in HepG2 cells **(Supplementary Figure 3B)**.

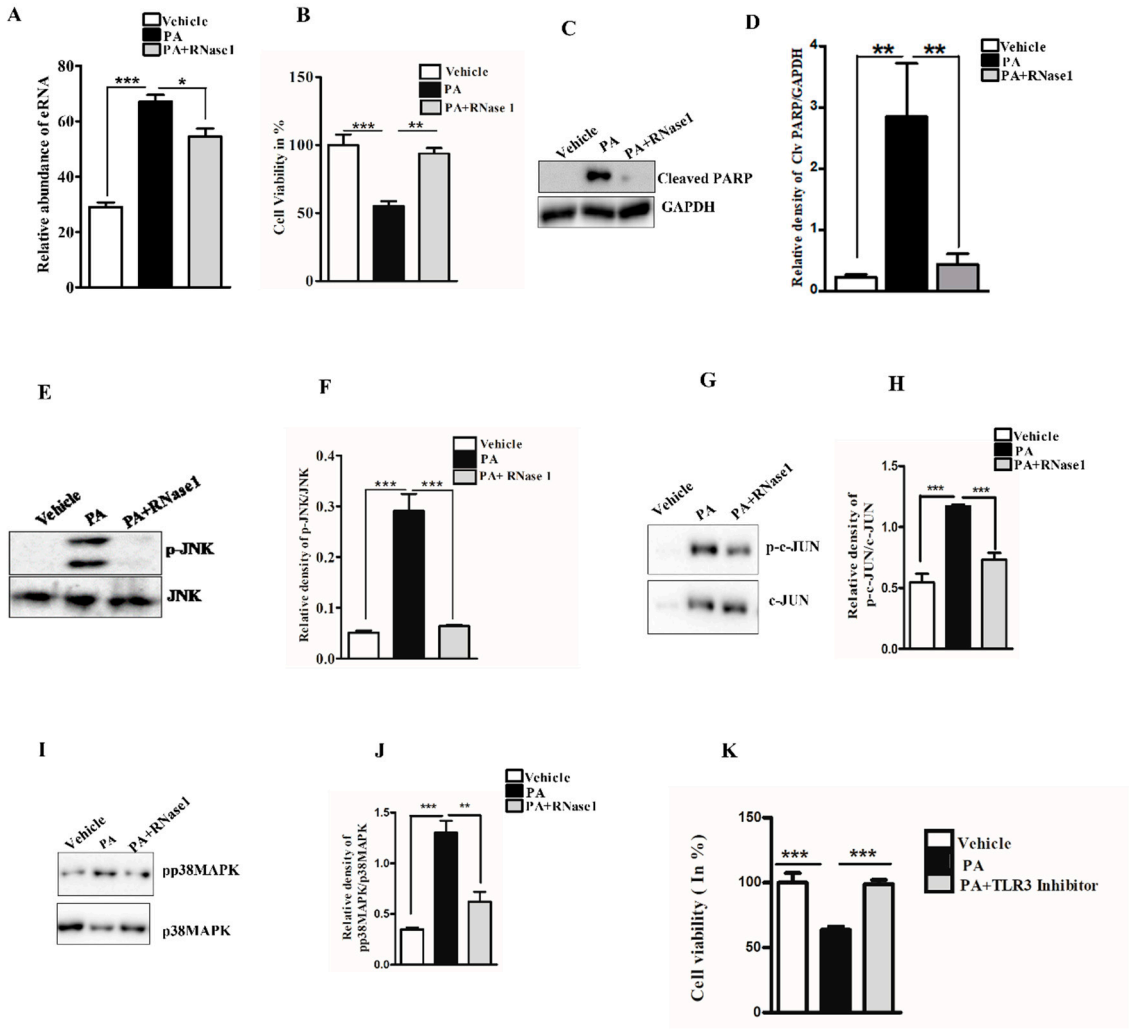

Figure 1. eRNA mediates lipotoxic injury in HepG2 cells (**A**) Relative abundance of eRNA in different experimental groups (Vehicle, PA, and PA+RNase 1). Values are mean ± SEM, n=5, ***p< 0.001 compares Vehicle to PA and *p < 0.05 compares PA to PA+ RNase 1. (**B**) % Cell viability shown through MTT assay among the three experimental groups. Data presented as mean ± SEM, n=5, ***p < 0.001 compares Vehicle to PA and **p< 0.01 compares PA to PA +RNase 1. (**C, D**) Representative immunoblots and densitometric analysis showing protein levels of cleaved PARP in different experimental groups. Values are mean ± SEM; n=5, **p< 0.01, compares Vehicle to PA and PA to PA+ RNase 1. (**E-J**) Representative immunoblots and densitometric analysis showing protein levels of p-JNK, p-c-JUN and p-p38MAPK in different experimental groups. Values are mean ± SEM, n=5, *p < 0.05, and ***p < 0.001, PA is compared to Vehicle and PA +RNase 1. (**K**) % Cell viability shown through MTT assay among Vehicle, PA and PA+TLR3 inhibitor treated HepG2 cells. Data presented as mean ± SEM, n=5 ***p < 0.001 compares Vehicle to PA and PA to PA +RNase 1.

PA is also known to increase mitochondrial dysfunction via its effect on mitochondrial reactive oxygen species (ROS) generation and loss of MMP [4]. Therefore, to investigate the effect of RNase 1 on PA induced mitochondrial damage, we first assessed the levels of mitochondrial ROS and

Preprints (www.preprints.org) | NOT PEER-REVIEWED | Posted: 20 June 2023 doi:10.20944/preprints202306.1436.v1

observed significant protection conferred by RNase 1 to PA induced mitochondrial ROS generation **(Figure 2A)**. Similarly, in agreement with its effect on mitochondrial ROS, RNase 1 prevented PA induced reduction in MMP, in HepG2 cells, as measured by JC-1 staining **(Figure 2B)**.

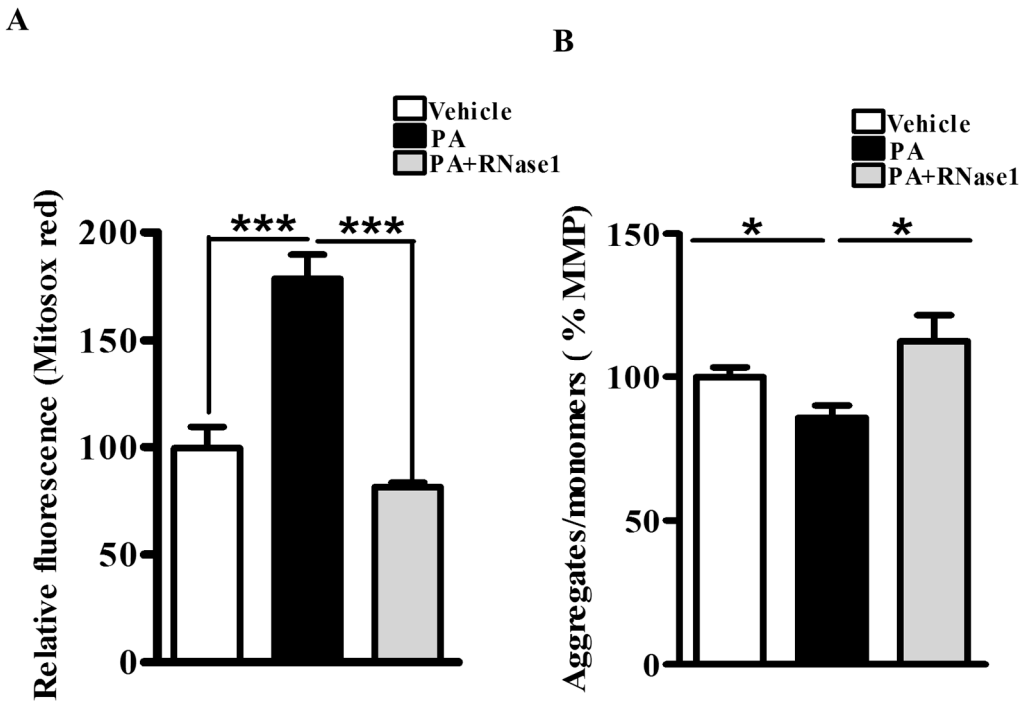

Figure 2. eRNA release is associated with mitochondrial dysfunction in HepG2 cells (**A**) MitoSox staining showing mitochondrial ROS generation in different experimental groups (Vehicle, PA, PA+RNase 1). Values are mean ± SEM, n=5, ***p < 0.001, PA is compared to Vehicle and PA +RNase 1 (**B**) JC-1 staining showing % MMP among the three experimental groups. Data presented as mean ± SEM, n=5 *p<0.05 compares Vehicle to PA and PA to PA +RNase 1.

Therefore, collectively these data indicate a direct involvement of eRNA in PA induced hepatic injury *in vitro* and the abrogation of these effects by RNase 1 treatment.

3.2. RNase 1 attenuates PA induced pro-inflammatory signalling in HepG2 cells

PA induced proinflammatory and pro-apoptotic signalling is linked to hepatic inflammation and cell death in NASH [30], and is associated with NF-κB activation [31]. Intriguingly, eRNA released from injured cells have been previously shown to induce TLR receptors and stimulate NF-κB dependent cytokine and chemokine synthesis [13]. Therefore, we speculated if PA induced cytokine production is partly mediated by eRNA signalling. To test this, we treated HepG2 cells with PA alone or PA along with RNase 1 and assessed the activation of NF-κB along with pro-inflammatory cytokine expression. Our results definitively showed that RNase 1 treatment almost completely inhibited PA induced NF-κB nuclear translocation, which measures its activation **(Figure 3A, B)**. In concurrence with NF-κB nuclear translocation, RNase 1 also prevented the PA induced activation of NF-κB transcriptional targets *IL-6* and *TNFα* in presence of PA **(Figure 3C)**. As *TNFα* is a major cell death inducer in hepatic cells [30], its inhibition may also explain the observed increase in the viability upon RNase 1 administration as described earlier **(Figure 1B)**. Similarly, the PA induced expression of several other NF-κB induced chemokines such as *CCL3, CCL20* and *CXCL10*, were repressed by RNase 1 co-treatment **(Figure 3D)**. Therefore, these data suggest an anti-inflammatory action of RNase 1 in hepatic cells treated with PA.

Preprints (www.preprints.org) | NOT PEER-REVIEWED | Posted: 20 June 2023 doi:10.20944/preprints202306.1436.v1

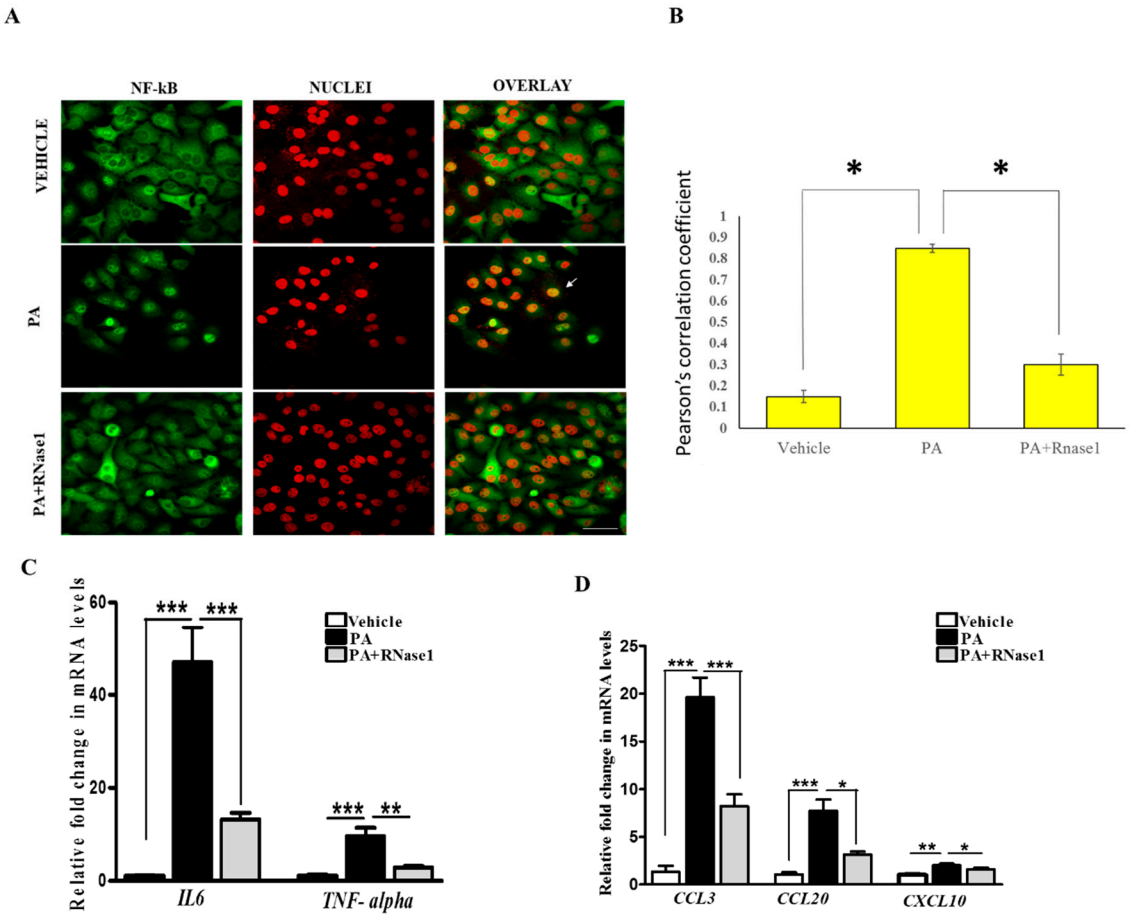

Figure 3. eRNA induces the expression of pro-apoptotic and pro-inflammatory cytokines in HepG2 cells (**A, B**) Representative immunofluorescence imaging and Pearson's correlation coefficient values showing colocalization of NFkB (green) and nuclei (red) in Vehicle, PA, and PA+RNase1 treated HepG2 cells cultured for 24 hours. Values are mean ± SD (n =5, *p < 0.05). Scale bar represents 10µm (**C**) Quantitative real-time polymerase chain reaction (qRT-PCR) analysis showing expression of pro-inflammatory cytokines (*TNF-α* and *IL6*) in VC, PA, and PA+RNase1 treated Hepg2 cells. Values are mean ± SEM, n=5, ***p < 0.001, PA is compared to Vehicle and PA +RNase 1. (**D**) qRT-PCR analysis of pro-inflammatory chemokines (*CCL3*, *CCL20* and *CXCL10*) in Vehicle, PA and PA+RNase1 treated Hepg2 cells. Data presented as mean ± SEM, n=5 *p < 0.05, **p< 0.01, and ***p < 0.001, PA is compared to Vehicle and PA +RNase 1.

3.3. RNase 1 administration mitigates NASH induced liver injury in mouse

To determine if eRNA is also involved in NASH pathogenesis *in vivo*, we used C57BL/6N mice and fed them HFMCD diet supplemented with 60 kcal% fat and 0.1% methionine by weight. These animal models rapidly developed severe NASH phenotype owing to the lipotoxic action of stored hepatic fat when compared to mice fed with control diet [32–34]. We administered RNase 1 in animals fed with HFMCD diet and followed its effects on the NASH phenotype. RNase 1 (50ug/kg), i.p. injections starting every alternate day after 2 weeks of HFMCD feeding were continued for the next 2 weeks. Mice fed either NCD or HFMCD diet for 4 weeks were taken for comparison. All the animals were sacrificed after 4 weeks.

Histological evaluation of the livers of mice fed with NC, HFMCD diet and HFMCD diet with RNase 1 intervention, showed a marked increase in hepatic steatosis in the HFMCD fed group, and its reduction upon RNase 1 co-administration **(Figure 4A)**. These results were further corroborated by hepatic TG measurement in the different experimental groups **(Figure 4B)**. HFMCD diet consumption damages hepatic tissue, which is reflected by the elevated levels of serum ALT in

Preprints (www.preprints.org) | NOT PEER-REVIEWED | Posted: 20 June 2023 doi:10.20944/preprints202306.1436.v1

HFMCD mice, consistent with histological findings **(Figure 4C)**. However, RNase 1 administration significantly reduced the levels of ALT in mice fed with HFMCD diet **(Figure 4C)**. Additionally, cellular stress markers such as p-JNK and p-p38MAPK which were upregulated in HFMCD fed mouse livers were also reduced by RNase 1 administration **(Supplementary Figure 4)**. Therefore, these results indicate a protective effect of RNase 1 on lipid induced liver injury *in vivo*.

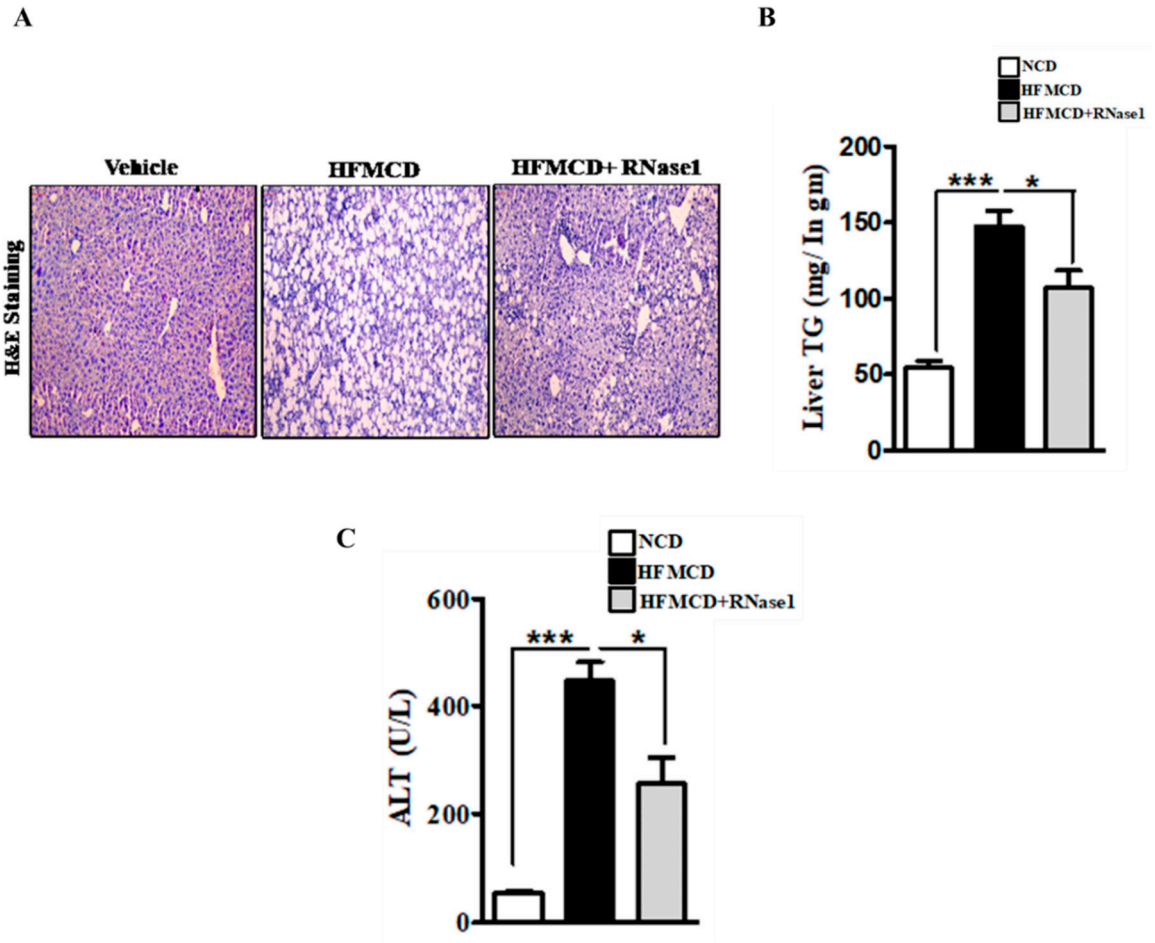

Figure 4. eRNA inhibition prevents NASH associated injury in mouse liver (A) Paraffin fixed liver sections stained with Hematoxylin/Eosin, showing hepatic steatosis in the three experimental groups, NCD, HFMCD and HFMCD+RNase1. **(B)** Hepatic TG levels from different experimental groups, NCD, HFMCD and HFMCD+RNase1.Values are mean ± SEM, n=5, *p < 0.05 and ***p < 0.001, HFMCD is compared to NCD and HFMCD + RNase 1. **(C)** Serum ALT levels from the three different experimental groups. Values are mean ± SEM, n=5, *p < 0.05 and ***p < 0.001, HFMCD is compared to NCD and HFMCD + RNase 1.

3.4. RNase 1 administration reduces NASH induced liver inflammation

The HFMCD mouse model mimics several aspects of human NASH pertaining to inflammation and immune cell infiltration [35]. Therefore, to validate our *in vitro* findings, we looked at the effect of RNase 1 on NASH induced NF-κB activation and pro-inflammatory cytokine expression. Our results demonstrated that similar to the effect of RNase 1 observed in HepG2 cells, *in vivo* blocking of eRNA action by RNase 1 significantly prevented hepatic NF-κB nuclear translocation **(Figure 5A, B)** and the expression of pro-inflammatory genes **(Figure 5C, D & Supplementary figure 5)** in the liver of HFMCD diet fed mice. Additionally, the mRNA expression of chemokines was also similarly altered by RNase 1 administration in the liver of HFMCD diet fed mice **(Figure 5E & Supplementary figure 5)**. Furthermore, we also observed an inhibitory effect of RNase 1 administration on intrahepatic macrophage infiltration in HFMCD diet fed mouse liver as assessed by hepatic F4/80

Preprints (www.preprints.org) | NOT PEER-REVIEWED | Posted: 20 June 2023 doi:10.20944/preprints202306.1436.v1

levels **(Figure 5F, G)**. Furthermore, the outcome of steatosis, inflammation, and hepatic ballooning, were assessed histologically by providing the NAFLD activity score, which was significantly decreased upon RNase 1 treatment **(Figure 5H)**. Collectively, these results demonstrated an anti-lipotoxic action of RNase 1 by attenuating NASH induced tissue damage and inflammation.

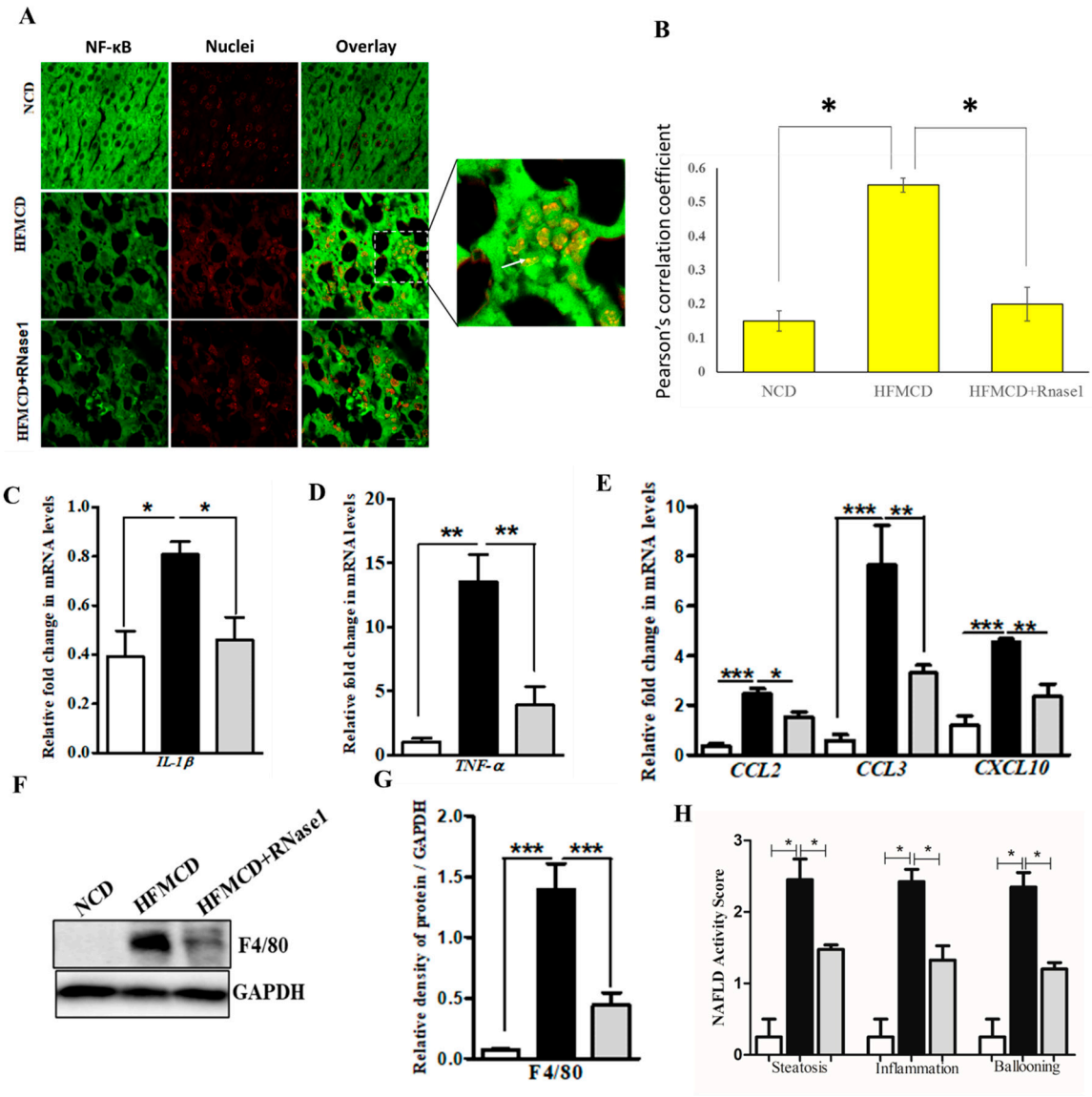

Figure 5. eRNA inhibition by RNase 1 attenuates cytokine production in NASH (A, B) Representative immunofluorescence imaging and Pearson's correlation coefficient values showing the colocalization NFkB (green) and nuclei (red) in in the liver sections of mice fed with NCD, HFMCD diet or HFMCD diet + RNase1.Values are mean ± SD (n =5, *p < 0.05). Scale bar represent 10μm. **(C, D)** qRT-PCR analysis showing expression levels of pro-inflammatory cytokines (*IL1β* and *TNF-α*) in the livers of mice fed with NCD, HFMCD diet or HFMCD diet + RNase1.Values are mean ± SEM, n=5, *p < 0.05 and **p < 0.01, HFMCD is compared to NCD and HFMCD+RNase1. **(E)** qRT-PCR analysis showing expression levels of some pro-inflammatory chemokines (*CCL2*, *CCL3* and *CXCL10*) in the livers of mice fed NCD, HFMCD diet or HFMCD diet + RNase1.Values are mean ± SEM, n=5, *p < 0.05, **p < 0.01, and ***p< 0.001, HFMCD is compared to NCD and HFMCD+RNase 1. **(F, G)** Representative immunoblot and densitometric analysis showing protein levels of F4/80 in different experimental groups. Values are mean ± SEM, n=5, ***p < 0.001, HFMCD is compared to NCD and HFMCD+RNase 1. **(H)** NAFLD activity score (NAS) in the three experimental groups, NCD, HFMCD and HFMCD+RNase1, Values are mean ± SEM, n=5, *p < 0.05, HFMCD is compared to NCD and

 doi:10.20944/preprints202306.1436.v1

HFMCD+RNase 1. In all the figures white bar represents NCD group, black bar represents HFMCD group and light grey bar represents HFMCD+RNase 1 group.

4. Discussion

As a disease, NAFLD displays a spectrum of disease stages ranging from benign steatosis to NASH [2], which is further presented as steatohepatitis, fibrosis and cirrhosis [1]. Unfortunately, despite its increasing prevalence across the globe, we still do not have an effective treatment strategy for NASH, other than life-style modifications [36]. At the molecular level, a tipping point during progression from benign steatosis to NASH, is the increase in the incidence of hepatocyte injury which is associated by necrotic/apoptotic death of hepatocytes, release of pro-inflammatory cytokines, and infiltration of macrophages leading to inflammation [37]. Therefore, understanding these events that link hepatocyte injury to inflammation is the key to preventing the transition and progression of steatosis to NASH.

One of the key concepts that help to explain the large spectrum of NAFLD seen in patients is the process called "Lipotoxicity" [37]. Indeed, when a liver cell experiences an increased flux of lipids, it attempts to store it into inert lipid droplets, however, in case the lipid load overruns the adaptive capacity of hepatocytes, the fatty acids inside the cells lead to the generation of reactive lipid species which trigger cell death by several distinct molecular mechanisms, encompassing the process of lipotoxicity [38]. Lipotoxic injury results in the release of DAMPs by hepatocytes, also known as danger signals that trigger the activation of sterile (i.e. in the absence of infection) inflammatory pathways, that when perpetuated over time, result in chronic injury and an abnormal wound healing response with fibrosis [39,40].

Basic and clinical research have provided evidence that the eRNA released by injured cells is an important player in the crosstalk between immunity and tissue injury in several diseases [13]. In fact, (patho-) physiological functions of eRNA are associated with, and in many cases, causally related to conditions such as arterial and venous thrombosis, atherosclerosis, ischemia/reperfusion injury, or tumor progression, especially in association with the elevated inflammatory status of these diseases [16,19,41–44]. eRNA can be liberated from the cells in a free form or bound to proteins or phospholipids as well as in association with extracellular vesicles (EVs) or apoptotic bodies [13]. Once released from an injured cell, eRNA binds to the adjacent cells via surface-bound Toll-like receptors (TLRs) and activates the pro-inflammatory NF-kB pathway, leading to the synthesis and secretion of pro-inflammatory cytokines like TNF-α and IL-6 [13]. Therefore, eRNA may serve as a catalyst to increase inflammatory environment and worsening of disease pathology. However, the adverse effects of eRNA are countered by several extracellular RNase, which proteolytically degrade eRNA [13]. In this regard, the exogenously administered RNase 1 bears considerable potential as new therapeutic agent, based on its tissue-protective functions that may translate into anti-inflammatory properties in different pathological situations [13].

As NASH represents a milieu wherein injured hepatocytes and cytokine production co-exist, it may be possible that eRNA drives NASH progression, however, this possibility has still not been tested so far. In the results presented here, we provide for the first-time, the direct evidence of eRNA acting as a paracrine pro-inflammatory mediator of lipotoxicity in hepatic cells. Our results demonstrate that inhibiting the biological activity of eRNA by RNase 1, prevents PA induced cellular stress in HepG2 cells as well as the expression of pro-inflammatory cytokines. Additionally, these data were confirmed in an animal model of NASH which showed that RNase 1 administration significantly reduced liver injury and inflammation associated with diet- induced NASH. Our study is in agreement with a previous report showing the possible involvement of TLR3 in human NASH, [45] which further strengthens our proposition of eRNA mediated inflammation in NASH.

Further studies are needed to profile eRNA across stratified NAFLD patients to assess the differences associated with the progression of the disease. Additionally, further experiments will be required to engineer stable RNase 1 with minimum side effects which can enter human clinical trials for NASH. In line with this, RNase therapy is already in clinical trials for cancer treatment [46].

Preprints (www.preprints.org) | NOT PEER-REVIEWED | Posted: 20 June 2023 doi:10.20944/preprints202306.1436.v1

Furthermore, based on our *in vitro* results, the use of specific TLR3 inhibitors should also be tested in preclinical models of NASH.

In summary, our results put forward eRNA released by injured hepatocytes under a lipotoxic environment constituting a feed forward loop, wherein hepatocyte injury is intertwined with the maintenance of a pro-inflammatory environment. Therefore, targeting eRNA by RNase 1 or specific TLR3/dsRNA inhibitors may be a new therapeutic strategy to reduce the pathogenesis of NASH **(Figure 6)**.

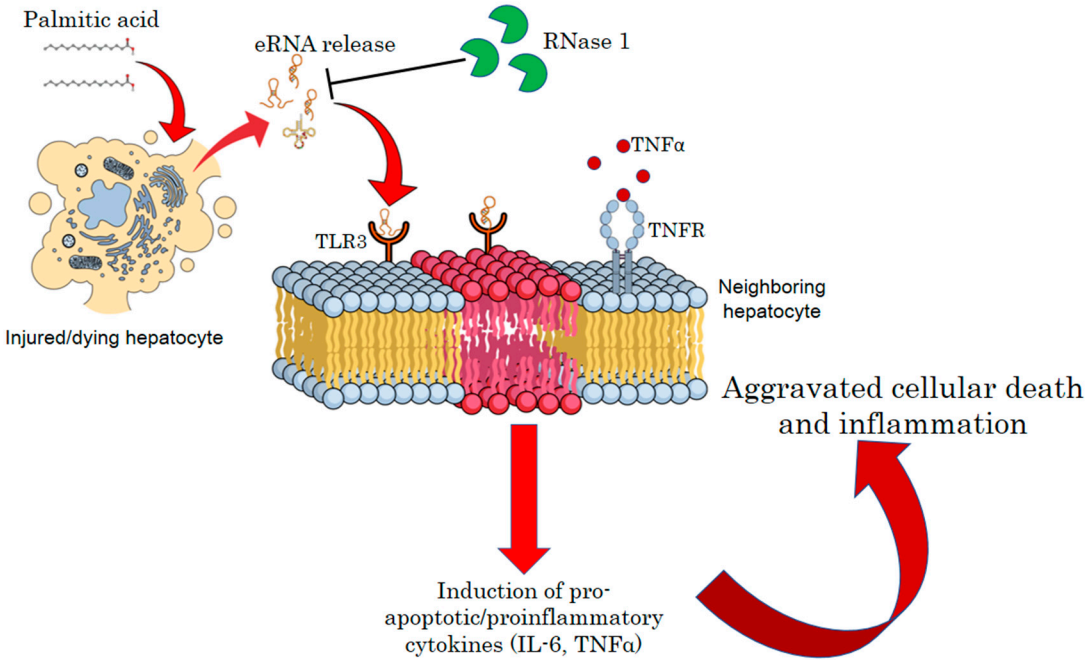

Figure 6. A schematic model of eRNA mediated lipotoxicity in hepatocytes. Release of eRNA from dying and injured hepatocytes upon lipotoxic insult by palmitic acid. These eRNAs bind to the TLR3 receptors on the plasma/endosomal membrane of neighboring hepatocytes, inducing pro-inflammatory cytokine signaling by activating IL6 and TNF-alpha, which in turn aggravates cellular death and inflammation in NASH.

5. Conclusions

Our results provide an insight into the pathological role of eRNA released by injured hepatocytes and put forth a proof-of-concept for limiting eRNA action to blunt NASH progression.

Supplementary Materials: The following supporting information can be downloaded at the website of this paper posted on Preprints.org, SuppleFigure S1: Effect of RNase 1 on hepatic cell viability.

Author Contributions: Conceptualization, R.A.S.; Methodology, A.T., S.R., Sana Raza; validation, A.T., S.R., Sana Raza, P.G., B.C., J.S.; formal analysis, A.T., S.R.; investigation, A.T., S.R.; writing—original draft preparation, A.T., C.P.C., R.A.S.; writing—review and editing, A.T., Sana Raza, R.A.S; supervision, R.A.S; funding acquisition, A.T., R.A.S. All authors have read and agreed to the published version of the manuscript.

Funding: This study was supported by the ICMR (2021-10209/CMB-BMS) Fellowship to A.T., DHR grant (YSS/2020/000009/PRCYSS) awarded to Sana Raza, SERB (CRG/2022/002149) and Wellcome Trust/DBT India Alliance Fellowship [IA/I/16/2/502691] awarded to R.A.S. This work in part constitutes the PhD thesis work of AT.

Institutional Review Board Statement: The animal study protocol was approved by the Institutional Animal Ethics Committee (IAEC), SGPGIMS, Lucknow (Project code: IAEC/P-054/30/2021 dated: 05/01/2022).

Data Availability Statement: The data presented in this study are available on request from the corresponding author.

Conflicts of Interest: The authors declare no conflict of interest.

References

1. Younossi, Z., et al., *Global Perspectives on Nonalcoholic Fatty Liver Disease and Nonalcoholic Steatohepatitis.* Hepatology, 2019. **69**(6): p. 2672-2682.
2. Sheka, A.C., et al., *Nonalcoholic Steatohepatitis: A Review.* JAMA, 2020. **323**(12): p. 1175-1183.
3. Engin, A.B., *What Is Lipotoxicity?* Adv Exp Med Biol, 2017. **960**: p. 197-220.
4. Fromenty, B. and M. Roden, *Mitochondrial alterations in fatty liver diseases.* J Hepatol, 2023. **78**(2): p. 415-429.
5. Svegliati-Baroni, G., et al., *Lipidomic biomarkers and mechanisms of lipotoxicity in non-alcoholic fatty liver disease.* Free Radic Biol Med, 2019. **144**: p. 293-309.
6. Mota, M., et al., *Molecular mechanisms of lipotoxicity and glucotoxicity in nonalcoholic fatty liver disease.* Metabolism, 2016. **65**(8): p. 1049-61.
7. An, P., et al., *Hepatocyte mitochondria-derived danger signals directly activate hepatic stellate cells and drive progression of liver fibrosis.* Nat Commun, 2020. **11**(1): p. 2362.
8. Handa, P., et al., *Mitochondrial DNA from hepatocytes as a ligand for TLR9: Drivers of nonalcoholic steatohepatitis?* World J Gastroenterol, 2016. **22**(31): p. 6965-71.
9. Luedde, T., N. Kaplowitz, and R.F. Schwabe, *Cell death and cell death responses in liver disease: mechanisms and clinical relevance.* Gastroenterology, 2014. **147**(4): p. 765-783.e4.
10. Mihm, S., *Danger-Associated Molecular Patterns (DAMPs): Molecular Triggers for Sterile Inflammation in the Liver.* Int J Mol Sci, 2018. **19**(10).
11. Shaker, M.E., *The contribution of sterile inflammation to the fatty liver disease and the potential therapies.* Biomed Pharmacother, 2022. **148**: p. 112789.
12. Wallace, S.J., et al., *Understanding the cellular interactome of non-alcoholic fatty liver disease.* JHEP Rep, 2022. **4**(8): p. 100524.
13. Preissner, K.T., S. Fischer, and E. Deindl, *Extracellular RNA as a Versatile DAMP and Alarm Signal That Influences Leukocyte Recruitment in Inflammation and Infection.* Front Cell Dev Biol, 2020. **8**: p. 619221.
14. Biswas, I., et al., *Extracellular RNA facilitates hypoxia-induced leukocyte adhesion and infiltration in the lung through TLR3-IFN-γ-STAT1 signaling pathway.* Eur J Immunol, 2015. **45**(11): p. 3158-73.
15. Cabrera-Fuentes, H.A., et al., *Regulation of monocyte/macrophage polarisation by extracellular RNA.* Thromb Haemost, 2015. **113**(3): p. 473-81.
16. Fischer, S., et al., *Self-extracellular RNA promotes pro-inflammatory response of astrocytes to exogenous and endogenous danger signals.* J Neuroinflammation, 2021. **18**(1): p. 252.
17. Grote, K., et al., *Extracellular Ribosomal RNA Acts Synergistically with Toll-like Receptor 2 Agonists to Promote Inflammation.* Cells, 2022. **11**(9).
18. Gruner, H.N. and M.T. McManus, *Examining the evidence for extracellular RNA function in mammals.* Nat Rev Genet, 2021. **22**(7): p. 448-458.
19. Kluever, A.K. and E. Deindl, *Extracellular RNA, a Potential Drug Target for Alleviating Atherosclerosis, Ischemia/Reperfusion Injury and Organ Transplantation.* Curr Pharm Biotechnol, 2018. **19**(15): p. 1189-1195.
20. Nation, G.K., C.E. Saffold, and H.H. Pua, *Secret messengers: Extracellular RNA communication in the immune system.* Immunol Rev, 2021. **304**(1): p. 62-76.
21. Preissner, K.T. and S. Fischer, *Functions and cellular signaling by ribosomal extracellular RNA (rexRNA): Facts and hypotheses on a non-typical DAMP.* Biochim Biophys Acta Mol Cell Res, 2023. **1870**(2): p. 119408.
22. Stieger, P., et al., *Targeting of Extracellular RNA Reduces Edema Formation and Infarct Size and Improves Survival After Myocardial Infarction in Mice.* J Am Heart Assoc, 2017. **6**(6).
23. Zechendorf, E., et al., *Ribonuclease 1 attenuates septic cardiomyopathy and cardiac apoptosis in a murine model of polymicrobial sepsis.* JCI Insight, 2020. **5**(8).
24. Zhang, X.Y., et al., *RNase attenuates acute lung injury induced by ischemia-reperfusion in mice.* Int Immunopharmacol, 2016. **40**: p. 288-293.
25. Brunt, E.M., et al., *Nonalcoholic steatohepatitis: a proposal for grading and staging the histological lesions.* Am J Gastroenterol, 1999. **94**(9): p. 2467-74.
26. Ji, J., et al., *Saturated free fatty acid, palmitic acid, induces apoptosis in fetal hepatocytes in culture.* Exp Toxicol Pathol, 2005. **56**(6): p. 369-76.
27. Gao, D., et al., *The effects of palmitate on hepatic insulin resistance are mediated by NADPH Oxidase 3-derived reactive oxygen species through JNK and p38MAPK pathways.* J Biol Chem, 2010. **285**(39): p. 29965-73.
28. Sinha, R.A., *Autophagy: A Cellular Guardian against Hepatic Lipotoxicity.* Genes (Basel), 2023. **14**(3): p. 553.
29. Cheng, K., X. Wang, and H. Yin, *Small-molecule inhibitors of the TLR3/dsRNA complex.* J Am Chem Soc, 2011. **133**(11): p. 3764-7.
30. Ezquerro, S., et al., *Ghrelin Reduces TNF-alpha-Induced Human Hepatocyte Apoptosis, Autophagy, and Pyroptosis: Role in Obesity-Associated NAFLD.* J Clin Endocrinol Metab, 2019. **104**(1): p. 21-37.
31. Joshi-Barve, S., et al., *Palmitic acid induces production of proinflammatory cytokine interleukin-8 from hepatocytes.* Hepatology, 2007. **46**(3): p. 823-30.
32. Matsumoto, M., et al., *An improved mouse model that rapidly develops fibrosis in non-alcoholic steatohepatitis.* Int J Exp Pathol, 2013. **94**(2): p. 93-103.

33. Rajak, S., et al., *Role of AKR1B10 and AKR1B8 in the pathogenesis of non-alcoholic steatohepatitis (NASH) in mouse.* Biochim Biophys Acta Mol Basis Dis, 2022. **1868**(4): p. 166319.
34. Rajak, S., et al., *Pharmacological inhibition of CFTR attenuates nonalcoholic steatohepatitis (NASH) progression in mice.* Biochim Biophys Acta Mol Basis Dis, 2023. **1869**(4): p. 166662.
35. Widjaja, A.A., et al., *Inhibiting Interleukin 11 Signaling Reduces Hepatocyte Death and Liver Fibrosis, Inflammation, and Steatosis in Mouse Models of Nonalcoholic Steatohepatitis.* Gastroenterology, 2019. **157**(3): p. 777-792 e14.
36. Vuppalanchi, R., et al., *Therapeutic pipeline in nonalcoholic steatohepatitis.* Nat Rev Gastroenterol Hepatol, 2021. **18**(6): p. 373-392.
37. Pierantonelli, I. and G. Svegliati-Baroni, *Nonalcoholic Fatty Liver Disease: Basic Pathogenetic Mechanisms in the Progression From NAFLD to NASH.* Transplantation, 2019. **103**(1): p. e1-e13.
38. Rada, P., et al., *Understanding lipotoxicity in NAFLD pathogenesis: is CD36 a key driver?* Cell Death Dis, 2020. **11**(9): p. 802.
39. Arguello, G., et al., *Recent insights on the role of cholesterol in non-alcoholic fatty liver disease.* Biochim Biophys Acta, 2015. **1852**(9): p. 1765-78.
40. Seki, E. and R.F. Schwabe, *Hepatic inflammation and fibrosis: functional links and key pathways.* Hepatology, 2015. **61**(3): p. 1066-79.
41. Kim, S., O.H. Jeon, and Y.J. Jeon, *Extracellular RNA: Emerging roles in cancer cell communication and biomarkers.* Cancer Lett, 2020. **495**: p. 33-40.
42. Noren Hooten, N., *Extracellular vesicles and extracellular RNA in aging and age-related disease.* Transl Med Aging, 2020. **4**: p. 96-98.
43. Hunter, R.W. and N. Dhaun, *Extracellular RNA in kidney disease: moving slowly but surely from bench to bedside.* Clin Sci (Lond), 2020. **134**(21): p. 2893-2895.
44. Giraldez, M.D., et al., *Phospho-RNA-seq: a modified small RNA-seq method that reveals circulating mRNA and lncRNA fragments as potential biomarkers in human plasma.* EMBO J, 2019. **38**(11).
45. Liu, H., et al., *TLR3/4 signaling is mediated via the NFkappaB-CXCR4/7 pathway in human alcoholic hepatitis and non-alcoholic steatohepatitis which formed Mallory-Denk bodies.* Exp Mol Pathol, 2014. **97**(2): p. 234-40.
46. Jordaan, S., et al., *Updates in the Development of ImmunoRNases for the Selective Killing of Tumor Cells.* Biomedicines, 2018. **6**(1).